



## Biological Activities Evaluation of Enantiopure Isoxazolidine Derivatives: In Vitro, In Vivo and In Silico Studies

Habib Mosbah<sup>1</sup> · Hassiba Chahdoura<sup>1</sup> · Asma Mannai<sup>2</sup> · Mejdi Snoussi<sup>2</sup> · Kaïss Aouadi<sup>3</sup> · Rui M. V. Abreu<sup>4</sup> · Ali Bouslama<sup>5</sup> · Lotfi Achour<sup>1</sup> · Boulbaba Selmi<sup>1</sup>

Received: 21 June 2018 / Accepted: 20 August 2018 / Published online: 31 August 2018  
© Springer Science+Business Media, LLC, part of Springer Nature 2018

### Abstract

A series of enantiopure isoxazolidines (**3a–c**) were synthesized by 1,3-dipolar cycloaddition between a (–)-menthone-derived nitron and various terminal alkenes. The screened compounds were evaluated for their antioxidant activity by two in vitro antioxidant assays, including  $\beta$ -carotene/linoleic acid bleaching, and inhibition of lipid peroxidation (thiobarbituric acid reactive species, TBARS). The results revealed that compound **3b** ( $EC_{50} = 0.55 \pm 0.09$  mM) was the most potent antioxidant as compared to the standard drug ( $EC_{50} = 2.73 \pm 0.07$  mM) using the TBARS assay. Furthermore, the antimicrobial activity was assessed using disc diffusion and microdilution methods. Among the synthesized compounds, **3c** was found to be the most potent antimicrobial agent as compared to the standard drug. Subsequently, the acute toxicity study has also been carried out for the newly synthesized compounds and the experimental studies revealed that all compounds were safe up to 500 mg/kg and no death of animals were recorded. The cytotoxicity of these compounds was assessed by the MTT cell proliferation assay against the continuous human cell lines HeLa and compound **3c** ( $GI_{50} = 46.2 \pm 1.2$   $\mu$ M) appeared to be more active than compound **3a** ( $GI_{50} = 200 \pm 2.8$   $\mu$ M) and **3b** ( $GI_{50} = 1400 \pm 7.8$   $\mu$ M). Interestingly, all tested compounds displayed a good  $\alpha$ -amylase inhibitory activity in competitive manner with  $IC_{50}$  values ranging between 23.7 and 64.35  $\mu$ M when compared to the standard drug acarbose ( $IC_{50} = 282.12$   $\mu$ M). In addition, molecular docking studies were performed to understand the possible binding and the interaction of the most active compounds to the  $\alpha$ -amylase pocket.

**Keywords** Enantiopure isoxazolidines · Antioxidant activity · Antimicrobial activity · Acute toxicity · Cytotoxicity ·  $\alpha$ -Amylase inhibition · Molecular docking

---

✉ Habib Mosbah  
mosbah\_habib@yahoo.fr

## Introduction

Heterocyclic compounds are the main class of cyclic organic compounds characterized by containing at least one heteroatom, the most common heteroatoms being nitrogen, oxygen and sulfur although other heterocyclic rings containing different heteroatoms are also known. Heterocycles have their significance in the field of pharmacy and industry. The concept of drug-like specie is very common in the field of medicinal chemistry; and the use of molecular descriptors found in already known drugs, to help in the planning the design of new molecules, is a broadly known strategy to exploit the chance of clinical success [1, 2].

Isoxazolidines are a class of powerful heterocycles [3], extensively used as precursors of 1,3-amino-alcohols or a various variety of natural compounds and derivatives [3], particularly amino acids [4, 5], alkaloids [6] and amino sugars [7]. Isoxazolidines possess interesting biological activities such as antioxidant [8, 9], antibacterial [9, 10], antifungal [11], antiretroviral [12] and antimycobacterial [13]. The 1,3-dipolar cycloaddition of nitrones and olefines is one of the most useful reactions for the synthesis of heterocyclic isoxazolidine derivatives [14]. These 1,3-dipolar cycloaddition reactions exhibit a high potential since they form cycloadducts with simultaneous creation of various chiral centers through highly stereocontrolled processes [15].

Recently, Ghannay et al. [10] have described the synthesis, the antioxidant, and the antimicrobial properties of enantiopure *N*-substituted pyrrolidin-2,5-dione derivatives obtained by 1,3-dipolar cycloaddition between chiral nitrone and *N*-substituted maleimides. More recently, Ghannay et al. [9] have reported the synthesis of novel enantiopure isoxazolidine derivatives by 1,3-dipolar cycloaddition of substituted aryl allyl carbonates, with a (–)-menthone-derived nitrone and the assessment of their in vitro antioxidant and antibacterial activities.

In view of all these facts, we report herein the synthesis of enantiopure isoxazolidine derivatives (**3a–c**) [4, 16] and the evaluation of some of their biological properties. The antioxidant activity of the synthesized compounds was measured by different in vitro assays, and antimicrobial activities were also evaluated by disc diffusion and microdilution methods. The acute toxicity of the enantiopure isoxazolidine derivatives (**3a–c**) on *Wistar* rats was also studied. The cytotoxic activity of compounds (**3a–c**) was tested using MTT cell proliferation assay. Finally, in vitro inhibition of diabetes key enzyme ( $\alpha$ -amylase) was evaluated and molecular docking studies were performed to provide insights on the possible binding manner and the interaction of these compounds with  $\alpha$ -amylase.

## Materials and Methods

### Chemicals Reagents and Enzymes

Iron (II) sulfate ( $\text{FeSO}_4$ ), thiobarbituric acid (TBA), trichloroacetic acid (TCA),  $\beta$ -carotene, linoleic acid, hydrochloric acid (HCl), sodium hydroxide (NaOH), acarbose, and porcine pancreatic amylase (PPA) were purchased from Sigma-Aldrich. NaCl was obtained from (Chemi Pharma, Tunisia). Hexane, chloroform, methanol, thin-layer chromatography (TLC) performed on silica gel 60F254, and gel column chromatography performed with silica gel Si 60 (40–63 mm) were purchased from Merck (Darmstadt, Germany); and all other chemicals used for the analyses were of analytical grade and were purchased from Sigma-Aldrich.

## General Procedure for the Synthesis of Novel Isoxazolidine Derivatives

Chiral nitrone **1** (0.84 mmol, 200 mg) and alkene (2.52 mmol) were dissolved in toluene (10 mL) and heated together at reflux for 48 h with good stirring. TLC showed the complete conversion of the chiral nitrone. The mixture was evaporated and the residue was purified by flash chromatography (EtOAc–PE 3:7) to afford desired compound **3**.

## Evaluation of the Antioxidant Activity

### $\beta$ -Carotene Bleaching Assay

In this test, oxidation of linoleic acid produces several oxidation products, which attack the chromophore of  $\beta$ -carotene, resulting in the bleaching of its characteristic color. However, the existence of antioxidant inhibits the  $\beta$ -carotene bleaching by the formed linoleic acid oxidation products. The capacity of the enantiopure isoxazolidine derivatives (**3a–c**) to prevent the bleaching of  $\beta$ -carotene was carried out as previously described by Condelli et al. [17] with a few modifications. In this assay,  $\beta$ -carotene (5 mg) was dissolved in 10 mL of chloroform (HPLC grade). Thereafter, 750  $\mu$ L of the obtained  $\beta$ -carotene solution, 33  $\mu$ L of linoleic acid, and 225 mg of Tween 40 were carefully mixed in round bottom flask. Then, the solvent was removed using a rotavapor. To obtain an emulsion, 75 mL of water was added slowly to the mixture and vigorously agitated. Aliquots (4 mL) of the emulsion (freshly prepared before each experiment) were transferred into test tubes containing 200  $\mu$ L of the enantiopure isoxazolidine derivatives (**3a–c**) serially diluted in ethanol to produce a test range of 0.03 to 2 mg/mL. Thereafter, the test tubes were incubated in a water bath at 50 °C for 2 h together with a negative control (blank) containing the same volume of ethanol instead of the sample. The absorbance was measured for all samples at 470 nm, immediately ( $t = 0$ ) and at after time of 120 min, using a spectrophotometer against a blank consisting of an emulsion without  $\beta$ -carotene. The percentage inhibition was calculated using the following formula:

$$I\% = (AS_{120\text{min}} - AC_{120\text{min}} / AC_{0\text{min}} - AC_{120\text{min}}) \times 100\%$$

where  $AS_{120\text{min}}$  is the absorbance of the sample at  $t = 120$  min,  $AC_{120\text{min}}$  is the absorbance of the control at  $t = 120$  min, and  $AC_{0\text{min}}$  is the absorbance of the control at  $t = 0$  min.

Samples were read against a blank containing the emulsion of  $\beta$ -carotene/linoleic acid. The isoxazolidine derivatives (**3a–c**) concentration (mg/mL) providing 50% inhibition ( $IC_{50}$ ) was calculated from the graph plotting antioxidant activity against synthesized compounds concentration. Trolox was used as a positive standard. All the tests were carried out for three sample replications and the results were averaged.

### Thiobarbituric Acid Reactive Species Assay

The ability of isoxazolidine derivatives (**3a–c**) to inhibit the products of lipid peroxidation was performed using TBARS quantification in homogenized sheep brain samples as described by Bellé et al. [18] with some modifications. The brain of sheep was homogenized with a polytron in ice-cold Tris-HCl buffer (20 mmol/L, pH 7.4) and was centrifuged at 3000 g during 10 min. An aliquot (100  $\mu$ L) of the recuperated supernatant was incubated with different concentrations (0.03 to 2 mg/mL) of the samples solutions (200  $\mu$ L) in the presence of 100  $\mu$ L  $FeSO_4$

(10 mmol/L) and 100  $\mu\text{L}$  ascorbic acid (0.1 mmol/L) at 37 °C for 1 h. Thereafter, to stop the reaction, 500  $\mu\text{L}$  of TCA (28% w/v) followed by 380  $\mu\text{L}$  of TBA, (2%, w/v) were added, and the mixture was then heated at 80 °C for 20 min. After centrifugation at 3000 g for 10 min, to remove the precipitated protein, the color intensity of the malondialdehyde (MDA)-TBA complex in the supernatant was measured at 532 nm. The inhibition ratio (%) was calculated using the following formula:

$$\text{Inhibition ratio (\%)} = \frac{[(\text{Abs}_C - \text{Abs}_S) / \text{Abs}_C] \times 100\%}{1}$$

where  $\text{Abs}_C$  and  $\text{Abs}_S$  were the absorbance (532 nm) of the control and the sample solution, respectively.

## Antimicrobial Activity

### Microorganisms

The target molecules were tested for antimicrobial activity against the following Gram-positive bacteria: *Staphylococcus aureus* ATCC 25923, *Staphylococcus epidermidis* CIP, *Bacillus cereus* ATCC 11778, *Listeria monocytogenes* CECT933, *Enterococcus faecalis* ATCC29212, and Gram-negative bacteria: *Vibrio parahaemolyticus* ATCC 17802, *Salmonella typhimurium* ATCC 1408, *Escherichia coli* ATCC 2592. On the other hand, the antifungal effect was tested against four *Candida* strains (*C. albicans* ATCC 2019, *C. krusei* ATCC 6258, *C. tropicalis* 06-085 and *C. parapsilosis* ATCC 22019).

### Disc-Diffusion Assay

The antimicrobial activity was investigated as described by Vuddhakul et al. [19] with minor modifications. In this assay, 10  $\mu\text{L}$  from the microorganisms culture stock was activated on a tube containing 9 mL of Mueller–Hinton (MH) broth (for bacteria) and Sabouraud (SB) chloramphenicol broth (for *Candida*), then incubated at 37 °C during 24 h. Cultures were then used for the antimicrobial activity of the isoxazolidine derivatives (**3a–c**), and the optical density was adjusted to  $10^7$  to  $10^8$  CFU/mL (0.1 at  $\text{OD}_{600}$  for bacteria and 0.4 at  $\text{OD}_{540}$  for *Candida* strains). The inoculums of bacteria and fungus were streaked onto MH and SB agar plates, respectively, using a sterile cotton swab, as recommended by the CA-SFM EUCAST 2017. Sterile filter discs (diameter 6 mm, Biolife Italy) were impregnated with 10  $\mu\text{L}$  of the isoxazolidine derivatives (**3a–c**) (2 mg/mL) and placed on the appropriate agar media. Ampicillin (10 mg/mL; 10  $\mu\text{L}$ /disc) and amphotericin B (10 mg/mL; 10  $\mu\text{L}$ /disc) were served as positive standards.

After 24 h of culture (37 °C), the diameter of the growth inhibition zone (IZ) was measured using a flat rule. Each experiment was carried out in triplicate and the mean value of the inhibition zones was registered. The results were expressed in terms of inhibition zone (IZ) of growth around each disc in millimeters as low activity (1–6 mm), moderate activity (7–10 mm), high activity (11–15 mm), and very high activity (12–20 mm) [20].

### Micro-Well Determination of MICs and MBCs/MFCs

The minimal inhibition concentrations (MICs) and the minimal bactericidal/fungicidal concentrations (MBCs/MFCs) values were deduced for all microbial strains as described by

Snoussi et al. [21] with some few modifications. The bacterial/fungal inoculums were prepared from 12-h broth cultures and suspensions and spectrophotometrically adjusted to  $10^7$  CFU/mL. The derivatives (**3a–c**) were first dissolved in ethanol (10%) and then serial twofold dilutions were made in a concentration range of 0.0018 to 2 mg/mL into 5 mL sterile glass tubes containing nutrient broth. Firstly, 95  $\mu$ L of nutrient broth was dispersed in each well of plates. An aliquot of 100  $\mu$ L from the stock solutions of each tested compound was added into the wells. Finally, 5  $\mu$ L from each microbial suspension was added to all the wells. The first well containing 195  $\mu$ L of nutrient broth (Mueller–Hinton broth or Sabouraud chloramphenicol broth) without isoxazolidine derivatives (**3a–c**) and 5  $\mu$ L of the inoculum corresponds to the negative control. The final volume in each well was 200  $\mu$ L. The plates were incubated during 24 h at 37 °C. The MIC was defined as the lowest concentration of the derivatives (**3a–c**) able to inhibit the growth of the microorganisms, so no visible changes were detected in the broth medium. The MBC/MFC ratio corresponds to the highest dilution of each sample, which exhibited clear fluid and an absence of visible growth.

## Experimental Animals

*Wistar* rats, weighing 160–180 g were recuperated from Pasteur Institute (Tunis, Tunisia). The animals were allowed free access to standard diet and water ad libitum. They were housed in cages and left for 2 days for acclimatization to animal room, maintained under controlled condition with an alternating 12 h light (L)/12 h dark (D) cycle (D/L/12:12 photoperiod at  $22 \pm 2$  °C). Before the day of administration, the animals were fasted overnight with free access to water. The animals were manipulated based on the guidelines of the Tunisian Society for the Care and Use of Laboratory Animals (ATSAL), and the protocol for the rat studies was approved by Institutional Animal Ethics of local Committee for Animal Care and Use.

## Acute Toxicity Studies

The oral acute toxicity of the isoxazolidine derivatives (**3a–c**) was carried out and the LD<sub>50</sub> value was determined. The laboratory rats were subjected to a fasting overnight prior to administration of the compounds. Two groups ( $n = 6$ ) were treated by oral administration of derivatives (**3a–c**) at different doses (200 and 500 mg/kg). The compounds (**3a–c**) were diluted in DMSO (maximum final concentration of 4%) and orally administered (per gavage). For the untreated group (negative control), distilled water was used with dose of 10 mL/kg. The positive control group received DMSO 4%. After the treatment period and for the first 4 h, the animals were carefully controlled for any toxic effect. Later, animals were observed during 14 days for any toxic effect or mortality [22]. The clinical observation was effected once a day to control the mortality, ill health or reaction to treatment, such as changes in fur and skin, eyes, behavior pattern, salivation, sleep, tremors, diarrhea, and coma.

On the sacrifice day, blood was withdrawn from all rats under urethane anesthesia. Thereafter, the blood in the plain test tube was allowed to stand for a minimum of 3 h to complete clotting. To recover the serum, the upper phase was recuperated and centrifuged at 4000 rpm at 4 °C for 10 min. The serums were then kept at  $-20$  °C until analysis for clinical biochemistry measurements using the enzymatic methods on an Integra 400 automaton (Roche Diagnostics, Mannheim, Germany). The clinical biochemistry values determination was for liver profile (alanine aminotransferase (ALT) and aspartate aminotransferase (AST)). Renal profile parameters measured were urea, creatinine, and CRP.

## Cytotoxic Activity

The cytotoxic effect of the derivatives (**3a–c**) was tested using MTT cell proliferation assay as described by Ben Mansour et al. [23]. Briefly, the continuous human cell lines HeLa (epithelial cervical cancer cell line) (ATCC, Manassas, VA, USA) were grown on different concentrations of the derivatives (**3a–c**). Forty-eight hours later, MTT was added. After 4 h of incubation, the formazan salts were dissolved and the OD was measured (570 nm). The results were expressed as GI<sub>50</sub> values, concentration that inhibited 50% of the net cell growth.

## In Vitro $\alpha$ -Amylase Inhibition Assay and Kinetics Study

The porcine pancreatic  $\alpha$ -amylase (PAA) activity was assessed using the dinitrosalicylic acid (DNS) method as described by Miller [24]. The reaction mixture contained 0.5 mL of appropriately diluted enzyme (2 U/mL) and 0.5 mL of buffer A (100 mmol/L MOPS pH 7; 3 mmol/L CaCl<sub>2</sub> and 10 mmol/L NaCl) containing 0.5% (w/v) of soluble starch. Maltose solution was used as reference to calculate the amylase activity.

To evaluate the inhibitory effects of the derivative compounds (**3a–c**) on  $\alpha$ -amylase, PPA was preincubated at room temperature (1 h) with different compounds concentrations (5 to 200  $\mu$ M). The reaction medium contained 20  $\mu$ L of the extract and 20  $\mu$ L of PPA. After incubation at 37 °C for 10 min, 1 mL of 3,5-dinitrosalicylic acid was added for the reaction mixture. At last, after incubation in a boiling water bath for 5 min, 10 mL of distilled water were added, and finally the absorbance was measured at 540 nm. A control tube was prepared similarly to the medium of the inhibition test but without compounds. For this assay, acarbose was used as a positive control. The PPA residual activity (RA %) was calculated as follows:

$$\text{RA (\%)} = A/B \times 100$$

where, *A* corresponds to the activity with inhibitor and *B* to the activity without inhibitor. The IC<sub>50</sub> values were calculated from plots of concentration of synthesized compounds versus percentage inhibition curves. The result is expressed as IC<sub>50</sub> (mg/mL), which corresponds to the compound concentration required to inhibit 50% of PPA activity. All tests were carried out in triplicate.

For the kinetic study, the reaction mixture was performed as described above, except that the substrate concentrations increased from 0.31 to 10 mM and in the presence of different concentrations of derivatives (**3a–c**). The results were used to construct Lineweaver–Burk plots to determine the type of inhibition, apparent Michaelis–Menten constant ( $K_m^{\text{app}}$ ) and maximum velocity ( $V_{\text{max}}$ ) values. The inhibition constant ( $K_i$ ) were determined plotting  $K_m^{\text{app}}$  vs. inhibitor concentration.

## Molecular Docking

Molecular docking has recently been established as an efficient technique for high throughput in silico screening of compounds' libraries. Molecular docking specifies the best positioning of a tested compound that interacts with the target protein, predicting the structure of a ligand within the constraints of a receptor binding site [25]. The chemoinformatics and computational chemistry increasingly plays a significant role in the initial examination of potential drug [26].

In this work, to explain the interactions between the derivatives (**3a–c**) and pancreatic  $\alpha$ -amylase, an *in silico* molecular docking study was established. To perform the docking studies, a PPA crystal structure was selected and obtained from the Protein Data Bank (PDB entry: 1HX0). The protein structure was prepared for docking by removing all waters and acarviosine-glucose that were co-crystallized with the structure. AutoDockTools1.5.2 (ADT) was then used to assign polar hydrogens, add Gasteiger charges, and save the protein structure in PDBQT file format [27]. A docking grid was selected using ADT in order to encompass the ligand binding site completely. The X,Y,Z grid center coordinates selected were 34.0, 20.0, and 53.3, respectively; and the X,Y,Z grid dimensions used were 30 by 30 by 30 Angstroms. The 2D structures of the studied derivative compounds (**3a–c**) were drawn using the ACD/ChemSketch Freeware 12.0 software. VegaZZ software was then used to perform 2D to 3D conversion and to save the structures in PDB file format [28]. Finally, ADT was used to convert PDB to PDBQT file format. All docking simulations were performed using AutoDock Vina software [29], using an exhaustiveness parameter of 32. Docking conformation analysis and image preparation were performed using PyMOL software [30].

## Statistical Analysis

The means and standard error (SEM) of data were calculated from independent experiments. Data analysis was performed using one-way ANOVA analyses followed by multi-range post hoc of Dunnett's test (comparison of control group with other groups). Statistical analyses were realized using GraphPad Prism and InStat softwares (GraphPad Software, La Jolla, USA). Graph Pad Prism was also used to fit sigmoid curves models. All statistical assays were two-tailed and ( $p < 0.05$ ) or less was then considered significant.

## Results and Discussion

### Chemistry

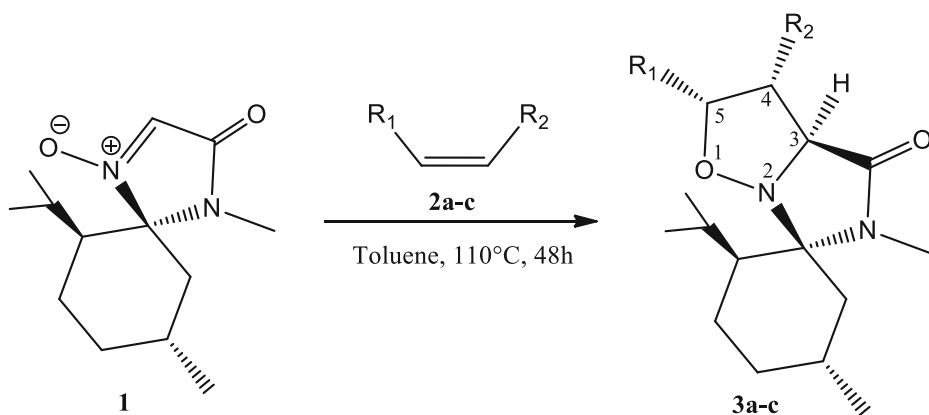
The chiral nitron **1** has been prepared from the (–)-menthone as reported earlier by Altenbach et al. [31]. The 1,3-dipolar cycloaddition of **1** with alkenes **2a–c** in refluxing toluene for 48 h afforded enantiopure isoxazolidines **3a–c** in good yields (Scheme 1 and Table 1). The stereoselectivity resulting from the approach of alkenes **2b–c** on the less hindered face of the spirocyclic nitron **1** has been discussed [4, 16]. The regioselectivity of the 1,3-dipolar cycloaddition reaction between **1** and **2a** has been reported [5, 31].

### Evaluation of Antioxidant Activity

It is obviously known that compounds with antioxidant properties could be expected to prevent some chronic human diseases and can lead to potentially effective drugs. To the best of our literature search, the synthesized enantiopure isoxazolidine derivatives are rarely reported for their antioxidant property [32].

In this work, the antioxidant activity of compounds **3a–c** was investigated by  $\beta$ -carotene bleaching and TBARS assays. The results were expressed as EC<sub>50</sub> values, with lower EC<sub>50</sub> values indicating higher antioxidant activity.





**Scheme 1** Synthesis of enantiopure isoxazolidines **3a–c**

As depicted in Table 2, using the  $\beta$ -carotene bleaching assay, the  $EC_{50}$  values for the different compounds (**3a–c**) ranged from  $0.73 \pm 0.08$  to  $1.67 \pm 0.12$  mM. The stronger antioxidant activity was obtained with compound **3b** which is about 3.6 times lower than that of the specific inhibitor Trolox ( $EC_{50} = 0.2 \pm 0.01$  mM) followed by **3a** and in lower degree **3c**.

Furthermore, our results show that the ability to inhibit the products of lipid peroxidation (TBARS assay) was very noticeable for all derivatives compounds (**3a–c**) than that obtained with the standard drug (Trolox). Results presented in Table 2 revealed that the  $EC_{50}$  value of compound **3b** was  $0.55 \pm 0.09$  mM which is fivefold lower compared to Trolox ( $2.73 \pm 0.07$  mM).

According to the two antioxidant assays, we can notice essentially that the compound **3b** ( $R_1: CH_2OH$ ,  $R_2: CH_2OH$ ) was the most active than other compounds. This interesting antioxidant activity may be related to the presence of two electron-donating groups ( $-CH_2OH$ ) as side chains. This observation is in accordance with the previous works [10, 32, 33] which confirm the interference of side chains of compounds on their biological properties.

## Antimicrobial Activity

Data on the antimicrobial activity of novel enantiopure isoxazolidine derivatives (**3a–c**) are reported in this work for the first time and are given as inhibition zone (IZ) diameters, MICs, MBCs, and MFCs (Tables 3 and 4). The antimicrobial activities of the target molecules were carried out using the agar diffusion and the microdilution methods on 12 test microorganisms, including 8 bacteria (5 Gram-positive and 3 Gram-negative) and 4 yeasts.

Our results show that the compounds were active against all the microbial strains, but in different degrees (Table 3). With the compound **3a**, the IZ varied from  $13.0 \pm 0.57$  to  $22.33 \pm 0.57$  mm, for bacterial strains, and from  $7.0 \pm 0.15$  to  $17.33 \pm 1.15$  mm for yeast strains. On the

**Table 1** Synthesis of enantiopure isoxazolidines (**3a–c**)

Entry	Compounds	$R_1$	$R_2$
1	<b>3a</b>	$CH_2OH$	H
2	<b>3b</b>	$CH_2OH$	$CH_2OH$
3	<b>3c</b>	$CH_2Cl$	$CH_2Cl$



**Table 2** Antioxidant activity of isoxazolidine derivatives (**3a–c**)

(EC <sub>50</sub> , mM)		
Compounds	$\beta$ -carotene bleaching	TBARS
(3a)	1.35 $\pm$ 0.11	0.81 $\pm$ 0.11
(3b)	0.73 $\pm$ 0.08	0.55 $\pm$ 0.09
(3c)	1.67 $\pm$ 0.12	1.40 $\pm$ 0.14
Trolox	0.2 $\pm$ 0.01	2.73 $\pm$ 0.07

Mean  $\pm$  SD,  $n = 3$ EC<sub>50</sub>, compound concentration corresponding to 50% of antioxidant activity

other hand, with the compound **3b**, the values of the IZ varied between 10.0  $\pm$  0.57 to 15.0  $\pm$  1.15 mm, for bacterial strains, and 7.0  $\pm$  0.15 to 20.33  $\pm$  0.57 mm for yeast strains. Finally, as listed in Table 3, we notice especially that the compound **3c** (R<sub>1</sub>:CH<sub>2</sub>Cl, R<sub>2</sub>: CH<sub>2</sub>Cl) appears the most active with the highest inhibition zones for the bacterial as well as the yeast strains. When using this compound (**3c**), *E. coli* ATCC 2592 appears the most sensitive bacteria, with IZ value of 26.0  $\pm$  1.15 mm which is about twofold higher than that measured with standard antibiotic (ampicillin). Similarly, *Candida krusei* ATCC 6258 was the most sensitive yeast, with IZ value of 24.66  $\pm$  1.01 mm which is about 2.2-fold higher than that measured with standard antibiotic (amphotericin B).

After the disk diffusion analyses, the active compounds were analyzed using an MIC assay to determine the lowest concentration able to inhibit visible bacterial growth. The MIC values listed in Table 4 revealed that all compounds **3a–c** had promising antimicrobial profiles against all tested bacteria strains with MICs (0.06–0.25 mg/mL) close to that observed for ampicillin used as standard antibiotic.

**Table 3** Antimicrobial activity of isoxazolidine derivatives (**3a–c**)

Microorganisms	Inhibition zones diameter (mm) <sup>a</sup>			
	(3a)	(3b)	(3c)	Ampicillin <sup>b</sup>
<b>Bacteria strains</b>				
<i>Staphylococcus aureus</i> ATCC 25923	22.33 $\pm$ 0.57	14.00 $\pm$ 0.1	24.00 $\pm$ 1.15	26.66 $\pm$ 0.57
<i>Bacillus cereus</i> ATCC 11778	15.00 $\pm$ 0.57	15.00 $\pm$ 1.15	17.00 $\pm$ 0.57	26.00 $\pm$ 1.00
<i>Staphylococcus epidermidis</i> CIP	19.00 $\pm$ 1.15	12.00 $\pm$ 0.57	20.00 $\pm$ 0.0	22.67 $\pm$ 0.57
<i>Enterococcus faecalis</i> ATCC 29212	17.00 $\pm$ 1.00	14.00 $\pm$ 1.00	21.00 $\pm$ 1.00	13.67 $\pm$ 0.57
<i>Listeria monocytogenes</i> CECT 933	13.00 $\pm$ 0.57	14.00 $\pm$ 0.57	14.00 $\pm$ 0.57	12.66 $\pm$ 0.57
<i>Escherichia coli</i> ATCC 2592	22.00 $\pm$ 1.15	13.00 $\pm$ 0.57	24.66 $\pm$ 1.01	11.67 $\pm$ 0.57
<i>Vibrio parahaemolyticus</i> ATCC 17802	18.00 $\pm$ 1.15	10.00 $\pm$ 0.57	20.00 $\pm$ 1.15	13.33 $\pm$ 0.57
<i>Salmonella typhimurium</i> ATCC 1408	16.00 $\pm$ 1.15	13.00 $\pm$ 1.15	15.00 $\pm$ 1.00	17.67 $\pm$ 1.15
<b>Yeast strains</b>	(3a)	(3b)	(3c)	Amphotericin B
<i>Candida albicans</i> ATCC 2019	7.00 $\pm$ 0.15	7.00 $\pm$ 0.15	14.00 $\pm$ 0.57	12.66 $\pm$ 0.57
<i>Candida krusei</i> ATCC 6258	17.33 $\pm$ 1.15	20.33 $\pm$ 0.57	26.00 $\pm$ 1.15	12.00 $\pm$ 0.00
<i>Candida tropicalis</i> 06–085	12.33 $\pm$ 0.57	14.33 $\pm$ 0.57	14.33 $\pm$ 0.57	1.00 $\pm$ 0.00
<i>Candida parapsilosis</i> ATCC 22019	15.33 $\pm$ 0.57	16.66 $\pm$ 0.57	21.66 $\pm$ 0.57	10.33 $\pm$ 0.57

The data are expressed as mean  $\pm$  SD ( $n = 3$ )<sup>a</sup> Diameter of inhibition zones of compound including diameter of well 6 mm<sup>b</sup> Ampicillin or amphotericin B was used as standard antibiotic at a concentration of 10 mg/mL

**Table 4** Determination of MIC, MBC and MFC (mg/mL) of the enantiopure isoxazolidines **3a–c**

Bacteria strains	Compound (3a)		Compound (3b)		Compound (3c)		Ampicillin	
	MIC <sup>a</sup>	MBC <sup>b</sup>	MIC <sup>a</sup>	MBC <sup>b</sup>	MIC <sup>a</sup>	MBC <sup>b</sup>	MIC <sup>a</sup>	MBC <sup>b</sup> / MFC <sup>c</sup>
<i>Staphylococcus aureus</i> ATCC 25923	0.125	0.25	0.25	1.00	0.25	1.00	0.25	0.40
<i>Bacillus cereus</i> ATCC 11778	0.125	0.25	0.06	0.25	0.25	1.00	0.25	0.40
<i>Staphylococcus epidermidis</i> CIP	0.125	0.25	0.125	0.50	0.125	0.50	0.011	12.00
<i>Enterococcus faecalis</i> ATCC 29212	0.125	0.25	0.125	0.50	0.125	0.50	0.023	0.093
<i>Listeria monocytogenes</i> CECT 933	0.125	0.25	0.125	0.50	0.125	0.50	0.023	0.093
<i>Escherichia coli</i> ATCC 2592	0.125	0.25	0.25	1.00	0.25	1.00	0.023	3.00
<i>Salmonella typhimurium</i> ATCC 1408	0.125	0.25	0.125	0.50	0.25	1.00	0.023	0.093
<i>Vibrio parahaemolyticus</i> ATCC 17802	0.25	0.50	0.125	0.50	0.25	0.50	0.011	3.00
Yeast strains	MIC <sup>a</sup>	MFC <sup>c</sup>	MIC <sup>a</sup>	MFC <sup>c</sup>	MIC <sup>a</sup>	MFC <sup>c</sup>	Amphotericin B	
<i>Candida albicans</i> ATCC 2019	0.125	0.50	0.25	0.50	0.25	1.00	0.024	0.781
<i>Candida krusei</i> ATCC 6258	0.125	0.50	0.25	0.50	0.50	1.00	0.09	0.195
<i>Candida tropicalis</i> 06–085	0.25	1.00	0.25	1.00	0.25	1.00	0.39	6.25
<i>Candida parapsilosis</i> ATCC 22019	0.50	1.00	0.125	0.25	0.50	1.00	0.195	0.39

<sup>a</sup> Minimal inhibitory concentration (mg/mL)

<sup>b</sup> Minimal bactericidal concentration (mg/mL)

<sup>c</sup> Minimal fungicidal concentration (mg/mL)

Thereafter, MBC or MFC which is the lowest concentration of compound or antibiotics that completely kills inoculated bacteria or fungi, respectively, was also determined. As depicted in Table 4, these values varied from 0.25 to 1 mg/mL for bacteria or yeasts and they are lower than those recorded with ampicillin or amphotericin particularly against *E. coli* ATCC 2592, *V. parahaemolyticus* ATCC 17802 and *Candida tropicalis* 06-085.

The difference in antimicrobial behavior of the tested compounds (**3a–c**) could be ascribed to the variation of susceptibility of the tested strains which may be related to their surface cells permeability to the tested derivatives. Also, this variation may be related to the solubility of these compounds in water [34, 35] and impermeability of the microorganism cells or differences between the ribosomes of microbial cells [36].

## Acute Toxicity Studies

### Physical Observation and Mortality

According to our toxicity study, no mortality of administered rats and no toxic effects were observed during the experimental period (14 days). Furthermore, the physical observation indicated that none of them exhibited signs of toxic effects, such as changes on skin, behavior pattern, salivation, tremors, diarrhea, sleep, and coma. Interestingly, no death also was recorded in both control and treated rats, suggesting that the LD<sub>50</sub> for chronic oral dosing with each of compounds was much higher than 500 mg/kg. According to the obtained LD<sub>50</sub> value, it can be suggested that the isoxazolidine derivatives (**3a–c**) should be considered as practically non-toxic in acute ingestion.

## Clinical Biochemistry

The clinical biochemistry (ALT, AST, urea, creatinine and CRP) results are summarized in Table 5. Interestingly, the clinical biochemistry parameters values were not significantly different ( $p > 0.05$ ) as compared to the control group. It is well known that transaminases (AST and ALT) are used as excellent indicators of liver function [37, 38]. It is also demonstrated that the lesion in the parenchymal cells of liver may increase the level of both transaminases in the blood. In addition, any increase in the level of AST in serum can be considered as a first sign of cell damage. We can deduce that the absence of significant differences in ALT and AST activities of the administered groups compared the control suggests that the chronic administration of compounds (3a–c) did not alter the hepatocytes and therefore the metabolism of the rats.

On the other hand, the level of creatinine and urea is well known as good indicators of the renal function [38]. Any damage in functional nephrons is generally marked by the increase of urea or creatinine levels [39]. Therefore, the results found in this study suggest that compounds (3a–c) did not also alter the renal function.

## Cytotoxic Activity

Cancer is a major health concern all around the world. Progresses in prevention and treatment of cancer have decreased the health rate, but the number of new diagnoses continues to increase. Therefore, new and more efficient anticancer agents are required to battle different cancer diseases. Furthermore, according to the various clinical studies [40, 41], it has been shown that compounds having the ability to block or suppress the proliferation of cancer cell by the induction of apoptotic cell death are considered as strong anticancer agents.

In our case, antiproliferative activity of isoxazolidine derivatives (3a–c) was evaluated in vitro by the estimation of cell growth effects on human cell lines HeLa (epithelial cervical

**Table 5** Effect of isoxazolidine derivatives (3a–c) on biochemical parameters of liver and kidney in rats measured during the acute toxicity study

Group	Treatment	AST (U/L)	ALT (U/L)	Urea (mmol/L)	Creatinine ( $\mu$ mol/L)	CRP (mg/L)
Group I	Negative control (distilled water)	118.42 $\pm$ 4.44	52.82 $\pm$ 2.45	7.02 $\pm$ 1.22	18.54 $\pm$ 1.12	47.28 $\pm$ 2.02
Group II	Positive control (DMSO 4%)	119.22 $\pm$ 4.12	51.06 $\pm$ 3.12	7.12 $\pm$ 1.02	17.88 $\pm$ 1.92	46.66 $\pm$ 4.22
Group III	Compound (3a) (200 mg/kg)	119.12 $\pm$ 4.81	50.22 $\pm$ 5.27	6.83 $\pm$ 0.71	18.46 $\pm$ 1.06	47.33 $\pm$ 5.04
	Compound (3b) (200 mg/kg)	120.45 $\pm$ 5.11	51.13 $\pm$ 4.27	6.74 $\pm$ 0.82	18.26 $\pm$ 1.12	47.13 $\pm$ 4.64
	Compound (3c) (200 mg/kg)	119.85 $\pm$ 4.66	52.02 $\pm$ 3.27	6.88 $\pm$ 1.08	17.91 $\pm$ 1.36	47.02 $\pm$ 3.68
Group IV	Compound (3a) (500 mg/kg)	118.80 $\pm$ 5.72	50.63 $\pm$ 4.50	7.01 $\pm$ 0.98	17.98 $\pm$ 2.02	47.19 $\pm$ 6.82
	Compound (3b) (500 mg/kg)	119.52 $\pm$ 4.37	51.10 $\pm$ 5.14	6.85 $\pm$ 0.94	18.50 $\pm$ 1.73	46.586.51
	Compound (3c) (500 mg/kg)	119.88 $\pm$ 4.80	51.76 $\pm$ 4.26	6.96 $\pm$ 1.08	17.98 $\pm$ 1.82	47.33 $\pm$ 3.62

ALT alanine aminotransferase, AST aspartate aminotransferase, CRP: C-reactive protein

cancer cell line). The results obtained are expressed as  $GI_{50}$ , which correspond to the concentration required to reach 50% of growth inhibition.

Ours results show that all derivatives have important toxicity to the cell type tested when compared to other studies [42, 43]. When comparing the  $GI_{50}$  values of compounds **3a–c**, compound **3c** ( $46.2 \pm 1.2 \mu\text{M}$ ) appeared to be more active against HeLa human cell lines than compounds **3a** ( $200 \pm 2.8 \mu\text{M}$ ) and **3b** ( $1400 \pm 7.8 \mu\text{M}$ ).

### **$\alpha$ -Amylase Inhibition Assay and Kinetics Study**

Carbohydrates are the main component of daily diet and play a key role in energy supply. The constituents of dietary carbohydrates should be cleaved into monosaccharides by the combined action of the two enzymes,  $\alpha$ -amylase and  $\alpha$ -glucosidase. The obtained monosaccharides can be absorbed from the lumen of intestine and thereafter circulated into the blood [44]. The inhibition of one or both enzymes ( $\alpha$ -amylase and  $\alpha$ -glucosidase) slows down the carbohydrates digestion and leads to decrease in blood glucose level and therefore it could be considered as a promising therapeutic way for the treatment of diabetes [45, 46].

All synthetic compounds (**3a–c**) were evaluated for their in vitro porcine pancreatic  $\alpha$ -amylase inhibitory activities at different concentrations and  $IC_{50}$  values were calculated (Fig. 1). A dose-dependent effect was observed upon increasing the concentrations of each compound and the maximum of inhibition (90%) was recorded with the compound **3c** at only  $165 \mu\text{M}$ . The results showed that all compounds exhibited potent inhibitory activity with  $IC_{50}$  values ranging between  $23.7$  and  $64.35 \mu\text{M}$  (Table 6) when compared to the standard drug acarbose ( $IC_{50} = 282.12 \mu\text{M}$ ).

The inhibition type of the isoxazolidine derivatives (**3a–c**) was determined using Lineweaver–Burk (double-reciprocal) plots as shown in Fig. 2a–c. For each compound, all lines had nearly the same y-intercept, while they had different slopes and x-intercepts, indicating that the type of inhibition was competitive. As shown by several researchers, in competitive inhibition, the inhibitor (compounds) and the substrate mutually and exclusively bind to the free enzyme, and therefore the inhibitor competes with the substrate for the free enzyme [47]. In fact, the competitive inhibition results of the three derivatives (**3a–c**) revealed that they all could occupy the active pocket of  $\alpha$ -amylase that bound to starch, thereby competitively inhibiting  $\alpha$ -amylase.

Furthermore, the inhibition constant ( $K_i$ ) for each inhibitor was determined by plotting  $K_m^{app}$  against inhibitor concentration. As reported in Table 6, compound **3c** ( $R_1: \text{CH}_2\text{Cl}$ ,  $R_2: \text{CH}_2\text{Cl}$ ) was the most effective inhibitor of  $\alpha$ -amylase followed by compound **3a** ( $R_1: \text{CH}_2\text{OH}$ ,  $R_2: \text{H}$ ) and compound **3b** ( $R_1: \text{CH}_2\text{OH}$ ,  $R_2: \text{CH}_2\text{OH}$ ) with  $K_i$  values of  $160.17$ ,  $574.32$ , and  $858.9 \mu\text{M}$ , respectively.

### **Structure-Based Docking Studies**

To better understand the molecular basis of compounds (**3a–c**) porcine pancreatic  $\alpha$ -amylase (PPA) inhibition activity, docking simulations using AutoDock Vina software were carried out against a known PPA protein structure (PDB code: 1HX0). In accordance with the experimental PPA inhibition results, compound **3c** presented the lowest predicted binding energy ( $\Delta G$ ) value of  $-8.3 \text{ Kcal/mol}$ , while compounds **3a** and **3b** presented higher  $\Delta G$  values of, respectively,  $-6.2$  and  $-6.3 \text{ Kcal/mol}$ . Since the predicted docking scores relate well with the

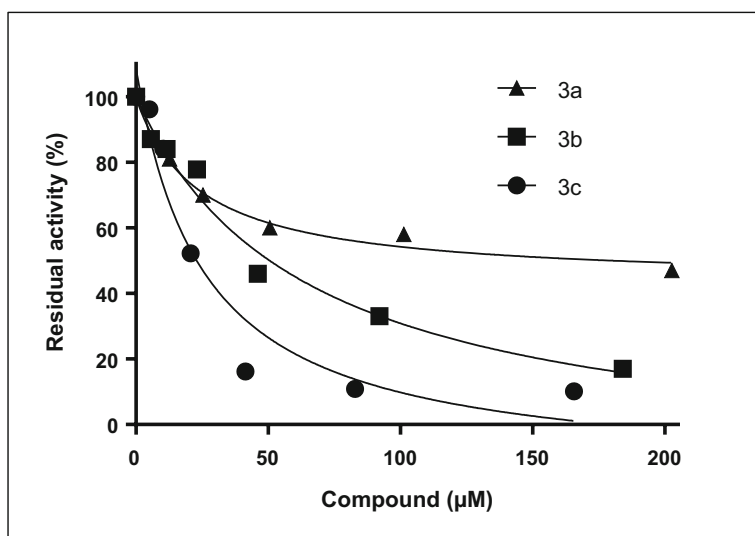


**Fig. 1** Residual  $\alpha$ -amylase activity at various concentrations of isoxazolidine derivatives (**3a–c**). Each point is the average value of three independent experiments

experimental results, we set out to analyze in more detail the predicted docking conformation of compound **3c**.

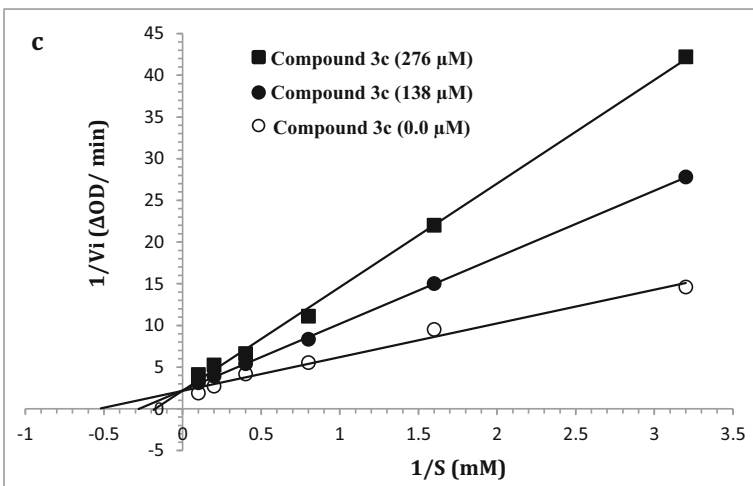
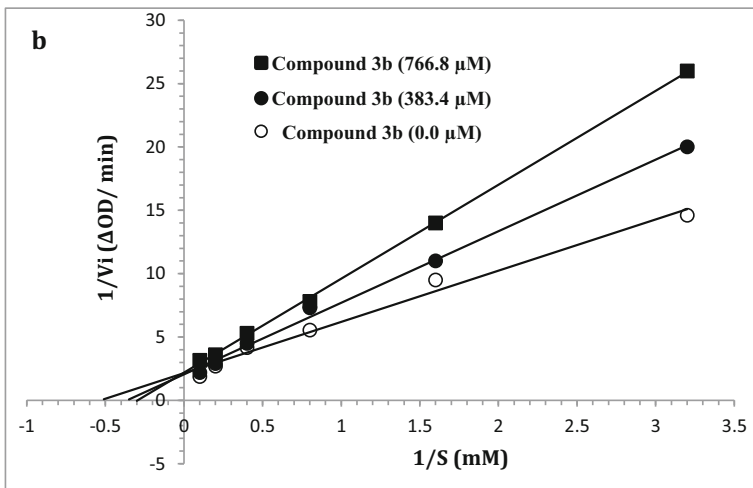
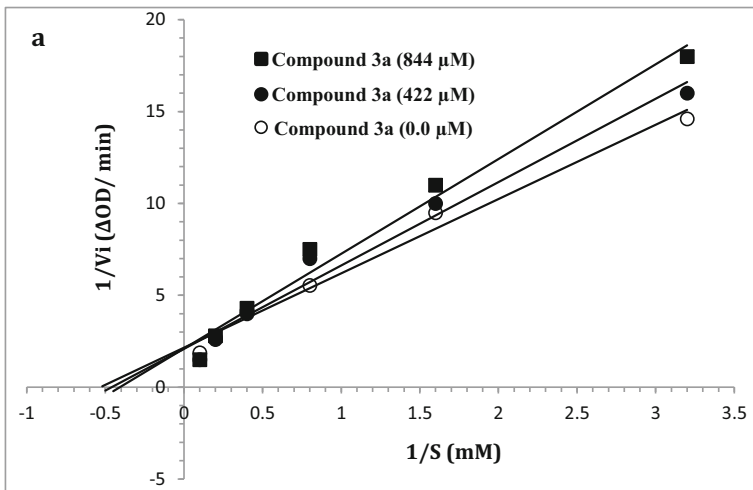
Figure **3a** displays the PPA structure used in the presented docking studies (PDB: 1HX0). In green color, we can observe acarviosine-glucose, the co-crystallized ligand that is bound to PPA catalytic site. Acarviosine-glucose is the smallest molecule of the trestatin family that inhibits PPA and yet is not hydrolyzed by the enzyme [48]. Superimposed to acarviosine-glucose is, in cyan color, the predicted docked conformation of compound **3c**. We can observe that compound **3c** fits nicely in the catalytic site of PPA. Figure **3b** shows compound **3c** predicted docked conformation in more detail. It is possible to observe that both chloride atoms and the carbonyl group oxygen present in compound **3c** structure are facing the solvent, probably being stabilized by hydrogen bonds, while the rings are positioned nicely in the different sub-pockets that comprise the complete PPA catalytic site. Taken together, the predicted binding energy and docked conformation of compound **3c** make a strong statement that the obtained docked conformation is probably the actual binding mode of compound **3c**.

## Conclusion

In summary, we have reported the synthesis of enantiopure isoxazolidine derivatives (**3a–c**) by 1,3-dipolar cycloaddition between a (–)-menthone-derived nitron and

**Table 6** Inhibitory effect of isoxazolidine derivatives (**3a–c**) on  $\alpha$ -amylase activity

Compound	IC <sub>50</sub> (μM)	K <sub>i</sub> (μM)	Inhibition mode
<b>(3a)</b>	25.56	574.32	Competitive
<b>(3b)</b>	64.35	858.9	Competitive
<b>(3c)</b>	23.7	160.17	Competitive



◀ **Fig. 2** Lineweaver–Burk plots of  $\alpha$ -amylase inhibition at different substrate [S] concentrations in absence or presence of various concentrations of compound **3a** (a), compound **3b** (b), and compound **3c** (c). Each point is the average value of three independent experiments

various alkenes. Some biological activities of the compounds were evaluated. The synthesized compounds display promising antimicrobial and antioxidant activities compared to the standard drugs. Regarding the antioxidant activities, all of the synthesized compounds were active and compounds **3b** ( $R_1$ :CH<sub>2</sub>OH,  $R_2$ : CH<sub>2</sub>OH) presented the best results in TBAS assay. Among these compounds, **3c** ( $R_1$ :CH<sub>2</sub>Cl,  $R_2$ : CH<sub>2</sub>Cl) showed notable antimicrobial activity with MIC and MBC values in the range of 0.25 to 1.0 mg/mL against all the tested strains. According to our results, the isoxazolidine derivatives (**3a–c**) should be considered as practically non-toxic in acute ingestion since any mortality of treated rats and no toxic effects were observed during the study period. All compounds exhibited superior  $\alpha$ -amylase inhibitory activity in the range of  $IC_{50}$  = 23.7 and 64.35  $\mu$ M as compared to standard acarbose ( $IC_{50}$  = 282.12  $\mu$ M). Molecular docking studies were carried out to better understand the molecular interaction of compounds with the active site of  $\alpha$ -amylase. Among these compounds, **3c** may potentially be developed as a new  $\alpha$ -amylase inhibitor for the treatment of type 2 diabetes.

Overall, although the number of derivatives in this work is reduced, the results of biological activities are very promising. Therefore, in the future, we attempt to the synthesis of the new isoxazolidine derivatives by systematic modification around our compounds with potent activities to produce drugs with higher therapeutic effect.

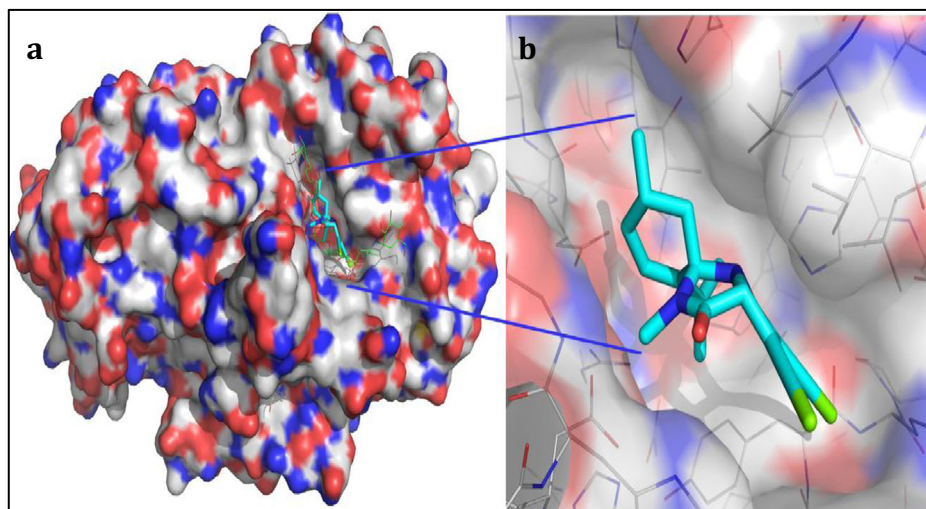


**Fig. 3** Representation of PPA structure with docking conformation of compound **3c**. **a** Surface representation of PPA with the co-crystallized acarviosine-glucose molecule (green color, wire representation) and the docked conformation of compound **3c** (cyan color, sticks and balls representation). **b** Detailed representation of compound **3c** predicted docked conformation



## Compliance with Ethical Standards

**Conflicts of Interest** The authors declare that they have no conflicts of interest.

## References

1. Taylor, R. D., MacCoss, M., & Lawson, A. D. G. (2014). Rings in drugs. *Journal of Medicinal Chemistry*, 57(14), 5845–5859.
2. Amara, M., Muhammad, S., Sumera, Z., Muhammad, S. S., Huma, A. B., Aamer, S., Izhar, H., & Jamshed, I. (2018). Synthesis, molecular modelling and biological evaluation of tetrasubstituted thiazoles towards cholinesterase enzymes and cytotoxicity studies. *Bioorganic Chemistry*, 78, 141–148.
3. Berthet, M., Cheviet, T., Dujardin, G., Parrot, I., & Martinez, J. (2016). Isoxazolidine: A privileged scaffold for organic and medicinal chemistry. *Chemical Reviews*, 116(24), 15235–15283.
4. Aouadi, K., Jeanneau, E., Msaddek, M., & Praly, J. P. (2007). New synthetic routes toward enantiopure (2S,3R,4R)-4-hydroxyisoleucine by 1,3-dipolar cycloaddition of a chiral nitron to C4 alkenes. *Synthesis*, 21, 3399–3405.
5. Aouadi, K., Jeanneau, E., Msaddek, M., & Praly, J. P. (2012). 1,3-Dipolar cycloaddition of a chiral nitron to (E)-1,4-dichloro-2-butene: A new efficient synthesis of (2S,3S,4R)-4-hydroxyisoleucine. *Tetrahedron Letters*, 53(23), 2817–2821.
6. Seerden, J. P. G., Boeren, M. M. M., & Scheeren, H. W. (1997). 1,3-dipolar cycloaddition reactions of nitrones with alkyl vinyl ethers catalyzed by chiral oxazaborolidines. *Tetrahedron*, 53(34), 11843–11852.
7. Frederickson, M. (1997). Optically active isoxazolidines via asymmetric cycloaddition reactions of nitrones with alkenes: Applications in organic synthesis. *Tetrahedron*, 53(2), 403–425.
8. Brahmi, J., Ghannay, S., Bakari, S., Kadri, A., Aouadi, K., Msaddek, M., & Vidal, S. (2016). Unprecedented stereoselective synthesis of 3-methylisoxazolidine-5-aryl-1,2,4-oxadiazoles via 1,3-dipolar cycloaddition and study of their *in vitro* antioxidant activity. *Synthetic Communications*, 46(24), 2037–2044.
9. Ghannay, S., Bakari, S., Msaddek, M., Vidal, S., Kadri, A., & Aouadi, K. (2018). Design, synthesis, molecular properties and *in vitro* antioxidant and antibacterial potential of novel enantiopure isoxazolidine derivatives. *Arabian Journal of Chemistry*. <https://doi.org/10.1016/j.arabjc.2018.03.013>.
10. Ghannay, S., Bakari, S., Ghabi, A., Kadri, A., Msaddek, M., & Aouadi, K. (2017). Stereoselective synthesis of enantiopure N-substituted pyrrolidin-2,5-dione derivatives by 1,3-dipolar cycloaddition and assessment of their *in vitro* antioxidant and antibacterial activities. *Bioorganic & Medicinal Chemistry Letters*, 27(11), 2302–2307.
11. Kumar, K. R. R., Mallesha, H., & Rangappa, K. S. (2003). Synthesis of novel isoxazolidine derivatives and their antifungal and antibacterial properties. *Archiv der Pharmazie -Pharmaceutical and Medicinal Chemistry*, 336, 159–164.
12. Loh, B., Vozzolo, L., Mok, B. J., Lee, C. C., Fitzmaurice, R. J., Caddick, S., & Fassati, A. (2010). Inhibition of HIV-1 replication by isoxazolidine and isoxazole sulfonamides. *Chemical Biology & Drug Design*, 75(5), 461–474.
13. Kumar, R. S., Perumal, S., Shetty, K. A., Yogeewari, P., & Sriram, D. (2010). 1,3-dipolar cycloaddition of C-aryl-N-phenylnitrones to (R)-1-(1-phenylethyl)-3-[(E)-arylmethylidene] tetrahydro-4(1H)-pyridinones: Synthesis and antimycobacterial evaluation of enantiomerically pure spiroisoxazolidines. *European Journal of Medicinal Chemistry*, 45(1), 124–133.
14. Nguyen, T. B., Martel, A., Gaulon-Nourry, C., Dhal, R., & Dujardin, G. (2012). 1,3-Dipolar cycloadditions of nitrones to heterosubstituted alkenes part 2: Sila-, thia-, phospho- and halosubstituted alkenes. *Organic Preparations and Procedures International*, 44(1), 1–81.
15. Nguyen, T. B., Martel, A., Gaulon, C., Dhal, R., & Dujardin, G. (2010). 1,3-dipolar cycloadditions of nitrones to heterosubstituted alkenes. Part 1: Oxa and aza-substituted alkenes. *Organic Preparations and Procedures International*, 42(5), 387–431.
16. Aouadi, K., Jeanneau, E., Msaddek, M., & Praly, J. P. (2008). Analogues of insulin secretagogue (2S,3R,4S)-4-hydroxyisoleucine: Synthesis by 1,3-dipolar cycloaddition reactions of chiral nitrones to alkenes. *Tetrahedron: Asymmetry*, 19(9), 1145–1152.
17. Condelli, N., Caruso, M. C., Galgano, F., Russo, D., Milella, L., & Favati, F. (2015). Prediction of the antioxidant activity of extra virgin oils produced in the Mediterranean area. *Food Chemistry*, 177, 233–239.

18. Bellé, N. A. V., Dalmolin, G. D., Fonini, G., Rubim, M. A., & Rocha, J. B. T. (2004). Polyamines reduces lipid peroxidation induced by different pro-oxidant agents. *Brain Research*, *1008*(2), 245–251.
19. Vuddhakul, V., Bhooponga, P., Hayeebilana, F., & Subhadhirasakulb, S. (2007). Inhibitory activity of Thai condiments on pandemic strain of *Vibrio parahaemolyticus*. *Food Microbiology*, *24*(4), 413–418.
20. Parveen, M., Ghalib, R. M., Khanam, Z., Mehdi, S. H., & Ali, M. (2010). A novel antimicrobial agent from the leaves of *Peltophorum vogelianum* (Benth.). *Natural Product Research*, *24*(13), 1268–1273.
21. Snoussi, M., Noumi, E., Trabelsi, N., Flamini, G., Papetti, A., & De Feo, V. (2015). *Mentha spicata* essential oil: Chimica composition: Antioxidant and antibacterial activities against planktonic and biofilm cultures of *Vibrio* spp. strains. *Molecules*, *20*(8), 14402–14424.
22. Walum, E. (1998). Acute oral toxicity. *Environmental Health Perspectives*, *106*(Suppl 2), 497–503.
23. Ben Mansour, R., Imtinen, B. H. J., Mohammed, B., Bochra, G., Nésrine, E., Hamadi, A., Zeineb, G. G., & Saloua, L. (2016). Phenolic contents and antioxidant activity of ethanolic extract of *Capparis spinosa*. *Cytotechnology*, *68*(1), 135–142.
24. Miller, G. L. (1959). Use of dinitrosalicylic acid reagent for determination of reducing sugar. *Analytical Chemistry*, *31*(3), 426–428.
25. Zaman, A., Muhammad, R., Sung-Yum, S., Mustafeez, M. B., & Najam-us-Sahar, S. Z. (2015). Synthesis, kinetic mechanism and docking studies of vanillin derivatives as inhibitors of mushroom tyrosinase. *Bioorganic & Medicinal Chemistry*, *23*, 5870–5880.
26. Yuriev, E., & Ramslund, P. A. (2013). Latest developments in molecular docking: 2010–2011 in review. *Journal of Molecular Recognition*, *26*, 215–239.
27. Morris, G.M., Huey, R., & Olson, A.J. (2008). "Using AutoDock for ligand-receptor docking." *Current Protocols in Bioinformatics Chapter 8: Unit 8.14*.
28. Pedretti, A., Villa, L., & Vistoli, G. (2004). VEGA - an open platform to develop chemo-bio-informatics applications, using plug-in architecture and script programming. *Journal of Computer-Aided Molecular Design*, *18*(3), 167–173.
29. Trott, O., & Olson, A. J. (2010). AutoDock Vina: Improving the speed and accuracy of docking with a new scoring function, efficient optimization, and multithreading. *Journal of Computational Chemistry*, *31*, 455–461.
30. Delano, W. L. (2002). "The PyMOL molecular graphics system." from <http://www.pymol.org>.
31. Altenbach, H.J., Kottenhahn, M., Vogt, A., Matthaus, M., Grundler, A., Hahn, M. (1997). Method of preparing optically active  $\alpha$ -amino acids and  $\alpha$ -amino acid derivatives. *Evonik Degussa GmbH*, 19533617 A1, and US Patent 6018050, 2000.
32. Mukherjee, S., Raunak, Dhawan, A., Poonam, Prasad, A. K., Olsen, C. E., Cholli, A. L., Errington, W., Raj, H. G., Watterson, A. C., & Prmar, V. S. (2004). Synthetic and biological activity evaluation studies on novel isoxazolidines. *Indian Journal of Chemistry*, *43*, 2670–2682.
33. Mubeen, M., Kini, S. G., & Pai, K. S. R. (2015). Design, synthesis, antioxidant and anticancer activity of novel pyrazole derivatives. *Der Pharma Chemica*, *7*, 215–223.
34. Kumar, A., Fernandes, J., & Kumar, P. (2014). Synthesis and biological evaluation of some novel isoxazolidine derivatives of carbostyryl. *International Journal of Pharmacy and Pharmaceutical Sciences*, *3*, 1267–1277.
35. Mondal, P., Jana, S., Balaji, A., Ramakrishna, R., & Kanthal, L. K. (2012). Synthesis of some new isoxazoline derivatives of chalconised indoline 2-one as a potential analgesic, antibacterial and anthelmintic agents. *Pharmaceutical Chemistry*, *4*, 38–41.
36. Colak, A., Terzi, U., Col, M., Karaoglu, S. A., Karabocek, S., Kucukdumlu, A., & Ayaz, A. (2010). DNA binding, antioxidant and antimicrobial activities of homo- and heteronuclear copper(II) and nickel(II) complexes with new oxime-type ligands. *European Journal of Medicinal Chemistry*, *45*(11), 5169–5175.
37. Rahman, M., Siddiqui, M. K., & Jamil, K. (2001). Effects of vepacide (*Azadirachta indica*) on asp artate and al anine aminotransferase profiles in a subchronic study with rats. *Human & Experimental Toxicology*, *20*(5), 243–249.
38. El Hilaly, J., Israili, Z. H., & Lyoussi, B. (2004). Acute and chronic toxicological studies of *Ajuga iva* in experimental animals. *Journal of Ethnopharmacology*, *91*(1), 43–50.
39. Lameire, N., Van Biesen, W., & Vanholder, R. (2005). Acute renal failure. *The Lancet*, *365*(9457), 417–430.
40. Frankfurt, O. S., & Krishan, A. (2003). Apoptosis-based drug screening and detection of selective toxicity to cancer cells. *Anti-Cancer Drugs*, *14*(7), 555–561.
41. Dinesh, M., Deepika, S., HarishKumar, R., Selvaraj, C. I., & Roopan, S. M. (2017). Evaluation of octyl- $\beta$ -D-glucopyranoside (OGP) for cytotoxic, hemolytic, thrombolytic, and antibacterial activity. *Applied Biochemistry and Biotechnology*, *185*, 450–463.
42. Iris Hall, H., Robert, A. I., Xiaoming, Z., Dwayne, L. D., Tyrone, W., Manik, L. D., Elaine, T., & Rosallah, A. M. (1997). Synthesis and cytotoxic action of 3,5-isoxazolidinediones and 2-isoxazolin-5-ones in murine and human tumors. *Archiv der Pharmazie*, *330*, 67–73.

43. Dorota, G. P., Marcin, C., Karolina, K., & Andrzej, E. W. (2011). Design, synthesis and cytotoxicity of a new series of isoxazolidine based nucleoside analogues. *Archiv der Pharmazie Chemie in Life Sciences*, *11*, 301–310.
44. Dewi, R. T., Iskandar, Y. M., Hanafi, M., Kardono, L. B. S., Angelina, M., Dewijanti, I. D., & Banjarnahor, S. D. S. (2007). Inhibitory effect of Koji *Aspergillus terreus* on  $\alpha$ -glucosidase activity and postprandial hyperglycemia. *Pakistan Journal of Biological Sciences*, *10*(18), 3131–3135.
45. Mahsa, R., Samaneh, J., Soheila, M., & Mahmood, R. M. (2014). Evaluation of alpha- amylase inhibition by *Urtica dioica* and *Juglans regia* extracts. *Iranian Journal of Basic Medical Sciences*, *17*, 465–469.
46. Montefusco-Pereira, C. V., de Carvalho, M. J., de Araújo Boleti, A. P., Teixeira, L. S., Matos, H. R., & Lima, E. S. (2013). Antioxidant, anti-inflammatory, and hypoglycemic effects of the leaf extract from *Passiflora nitida* Kunth. *Applied Biochemistry and Biotechnology*, *170*(6), 1367–1378.
47. Copeland, R. A. (2013). *Evaluation of enzyme inhibitors in drug discovery: A guide for medicinal chemists and pharmacologists* (2nd ed.). New Jersey: Wiley (Chapter 3).
48. Qian, M., Nahoum, V., Bonicel, J., Bischoff, H., Henrissat, B., & Payan, F. (2001). Enzyme-catalyzed condensation reaction in a mammalian alpha-amylase. High-resolution structural analysis of an enzyme-inhibitor complex. *Biochemistry*, *40*(25), 7700–7709.

## Affiliations

**Habib Mosbah<sup>1</sup> · Hassiba Chahdoura<sup>1</sup> · Asma Mannai<sup>2</sup> · Mejdi Snoussi<sup>2</sup> · Kaïss Aouadi<sup>3</sup> · Rui M. V. Abreu<sup>4</sup> · Ali Bouzlama<sup>5</sup> · Lotfi Achour<sup>1</sup> · Boulbaba Selmi<sup>1</sup>**

<sup>1</sup> Laboratory of Bioresources, Integrative Biology and Valorization, Higher Institute of Biotechnology of Monastir, University of Monastir, Avenue Taher Hadded BP 74, 5000 Monastir, Tunisia

<sup>2</sup> Laboratory of Genetic, Biodiversity and Valorization of Bioresources, Higher Institute of Biotechnology of Monastir, University of Monastir, Avenue Taher Hadded BP 74, 5000 Monastir, Tunisia

<sup>3</sup> Laboratory of Heterocyclic Chemistry, Natural Products and Reactivity, Faculty of Sciences of Monastir, University of Monastir, Avenue de l'Environnement, 5000 Monastir, Tunisia

<sup>4</sup> Mountain Research Center (CIMO), ESA, Polytechnic Institute of Bragança, Bragança, Portugal

<sup>5</sup> Biochemistry Department, LR12SP11, Sahloul University Hospital, 4054 Sousse, Tunisia